Kayt E. Frisch
Department of Engineering,
Dordt College,
498 4th Ave SE,
Sioux Center, IA 51250
e-mail: kayt.frisch@dordt.edu

David Marcu
Sauk Prairie Memorial Hospital,
Prairie du Sac, WI 53578
e-mail: dmarcu@spmh.org

Geoffrey S. Baer
Department of Orthopedics and Rehabilitation,
University of Wisconsin,
Madison, WI 53705
e-mail: baer@ortho.wisc.edu

Darryl G. Thelen
Department of Biomedical Engineering,
Department of Mechanical Engineering,
University of Wisconsin,
Madison, WI 53705
e-mail: thelen@engr.wisc.edu

Ray Vanderby
Departments of Orthopedics and Rehabilitation
and Biomedical Engineering,
University of Wisconsin,
Madison, WI 53705
e-mail: Vanderby@ortho.wisc.edu

The Influence of Partial and Full Thickness Tears on Infraspinatus Tendon Strain Patterns

Tears on the bursal and articular sides of the rotator cuff tendons are known to behave differently and strain is thought to play a role in this difference. This study investigates the effect of tear location on the changes in three strain measurements (grip-to-grip, insertion, and mid-substance tissue) in a sheep infraspinatus tendon model during axial loading. We introduced a 14 mm wide defect near the insertion from either the articular or bursal side of the tendon to three depths (3 mm, 7 mm & full) progressively. For each condition, tendons were sinusoidally stretched (4% at 0.5 Hz) while insertion and mid-substance strains were tracked with surface markers. For a fixed load, grip-to-grip strain increased significantly compared to intact for both cuts. Insertion strain increased significantly for the bursal-side defect immediately but not for the articular-side until the 66% cut. Mid-substance tissue strain showed no significant change for partial thickness articular-side defects and a significant decrease for bursal-side defects after the 66% cut. All full thickness cuts exhibited negligible mid-substance tissue strain change. Our results suggest that the tendon strain patterns are more sensitive to defects on the bursal side, and that partial thickness tears tend to induce localized strain concentrations in regions adjacent to the damaged tissue. [DOI: 10.1115/1.4026643]

Keywords: tendon, mechanics, rotator cuff

1 Introduction

Rotator cuff tendon tears are a common shoulder ailment that can substantially diminish one's ability to perform routine tasks [1,2]. However, the severity, location and treatment of tears within the rotator cuff tendons can vary considerably. For example, rotator cuff tears can be either partial or full thickness, and can be located on either the bursal or the articular side of the tendon (and occasionally intra-substance). Partial thickness tears are thought to be more common than full thickness tears, affecting between 6% and 37% of the general population [3,4]. No consistent guidelines for treating partial thickness rotator cuff tears currently exist. Most studies recommend a minimum of three to six months of physical therapy (conservative treatment) before considering surgery [3,5]. As a general rule, tears are then surgically repaired if they are greater than 50% of the thickness of the tendon [6–8]. Bursal-sided tears tend to respond poorly to physical therapy, prompting some surgeons to forego long periods of conservative therapy and instead repair bursal-sided tears earlier [5].

Ex vivo models have been used to better understand the mechanics of rotator cuff tear formation and propagation by measuring strain variations in response to external loading [9,10]. Studies have shown there is a strain differential between the bursal and articular sides of the tendon, with the majority reporting that strain is greater on the bursal side of intact tendon [10–12]. These strain differentials may reflect differences in stiffness between the bursal and articular sides of the tendon [13,14]. This stiffness difference may contribute to the clinical observation that intra-substance tears tend to propagate between the bursal and articular layers [4]. It has also been observed that larger defects lead to greater localized strain in the tendon [9]. Furthermore, measuring both whole-tendon and tissue strains for defects of varying thickness supports the repair criterion that surgical repair should be performed for defects greater than 50% of the thickness, since strain significantly increased when the tears reached half the thickness [15,16]. Despite the clinical relevance, prior studies have not directly compared strain patterns resulting from tears that originate on opposite sides of the tendon.

The goal of this study is to investigate the effect of tear location on the changes in tissue strains experienced by the rotator cuff tendons during loading (Fig. 1). As a result of the reported stiffness differences between layers, we hypothesized that defects initiated on the bursal side of the tendon will increase the overall tendon strain more than similar articular-sided defects [12,13]. We also hypothesized that localized strains in tissue adjacent to the defect (in the load-bearing direction of the tendon) will decrease due to unloading on the cut side of the tendon, while tissue strains on the surface opposite from the cut will increase since they will be carrying a greater proportion of the load. To test these hypotheses, we introduced tears in to either the bursal or articular side of sheep infraspinatus tendons (a commonly used model for the human supraspinatus tendon owing to the similarities in size and anatomy between the two species) and then assessed the effect of tear placement on localized tendon strains during tensile loading [17,18].

2 Experimental Methods

2.1 Study Design. Sixteen forelimbs (including the scapula) were collected from skeletally mature female sheep that had been euthanized for an unrelated study.

Contributed by the Bioengineering Division of ASME for publication in the JOURNAL OF BIOMECHANICAL ENGINEERING. Manuscript received August 16, 2013; final manuscript received January 17, 2014; accepted manuscript posted February 6, 2014; published online April 10, 2014. Assoc. Editor: Kristen Billiar.

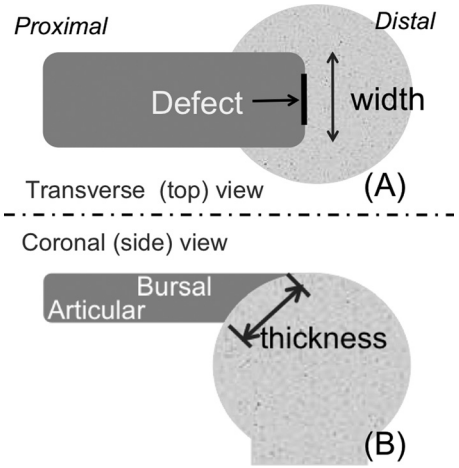

Fig. 1 The width and thickness designations used for tendon defect creation. (*a*) The top view of the tendon showing the width of the tendon and indicating the position of the small and large defects. (*b*) The side view of the tendon, indicating bursal and articular sides of the tendon and the thickness across the footprint.

2.2 Specimen Preparation. The infraspinatus tendon and humerus were removed from each limb, and care was taken to leave the tendon-bone insertion site intact. The muscle fibers were dissected from the proximal end of the tendon. During the preparation process, the tendons were kept moist in physiologic buffered saline. Specimens were stored at −80 °C until testing [19]. At the time of testing, specimens were thawed in warm water for half an hour. The long bone portion of the humerus was removed from the bone-tendon unit and a hole was drilled in the humeral head perpendicular to the tendon insertion for mounting in the test frame. The width and thickness of the tendon insertion were measured using digital calipers and the cross-sectional area of the insertion site was calculated assuming an elliptical footprint on the bone. The cross-sectional area of the free tendon was similarly obtained.

2.3 Mechanical Testing. Tensile testing was performed using a servo-hydraulic mechanical test system (Bionix 858, MTS, Minneapolis, MN) with the tendon mounted in a bath (Fig. 2). The bony end of the tendon was fixed to an L-shaped bracket via a post that was placed through a hole drilled in the humeral head. Cleats were placed on the vertical surface of the bracket to keep the bone-tendon unit from rotating during testing. The soft tissue end was secured in a moveable grip attached to the load cell. Specimens were mounted so that fibers were loaded

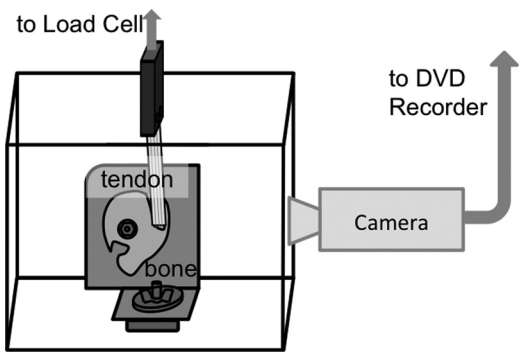

Fig. 2 Sheep infraspinatus tendon optical test setup. Sheep infraspinatus bone-tendon segments were mounted in a custom bath affixed to a servo-hydraulic mechanical testing machine.

visually aligned and taut upon onset of loading, resulting in approximately a 15 deg angle between the bone and the tendon. Grip-to-grip displacement was controlled by the servo-hydraulic testing system and the resulting load was measured with a 500 lb load cell (Eaton Corporation, Cleveland, OH). Once mounted in the loading frame, tendons were preloaded to 2 N to remove slack. Following preloading, tendons were preconditioned using a sinusoidal stretch (1 Hz) to 2% strain (based on length at preload) for 10 s, then allowed to rest for 500 s to ensure adequate recovery between tests. Subsequent mechanical testing was performed by subjecting tendons to a cyclic peak tensile displacement at 4% strain for 10 cycles at 0.5 Hz with a rest of 500 s between each test. Testing was performed for each of the four defect conditions. To avoid strain history-dependent effects, only the last three cycles were used for analysis.

2.4 Defect Creation. Defects mimicking both partial and full thickness avulsion tears were created near the tendon-bone insertion by using a custom-designed 14 mm wide razor blade mounted on a polycarbonate block which was positioned to prevent the blade from cutting deeper than desired. All tendons in this study had similar thicknesses (average 19 ± 1.2 mm), so defects were created using a constant depth. After testing the intact tendon to obtain a set of baseline load and displacement measurements, a 3 mm deep defect (approximately 33% of the thickness of the insertion) was created at the bone-tendon interface in the center of either the bursal or the articular surface of the tendon (Fig. 1). After mechanical testing had been performed, the existing defect was deepened to 7 mm (approximately 66% of the thickness of the insertion) and mechanical testing was repeated. Finally, the defect was deepened so that it was through the full thickness of the tendon, leaving the tendon attached only at the anterior and posterior edges and mechanical testing was again repeated. Specimens were randomly assigned to either the bursal or articular groups, so that half of the defects were created from the bursal side of the tendon and half of the defects were created from the articular side of the tendon.

2.5 Strain Calculations. A grid of custom graphite-impregnated silicon markers was placed on the bursal surface of the bone and tendon to measure tissue motion during the mechanical testing (Fig. 3). Each test was recorded using a black and white video camera (30 fps, Sony Corporation, New York, NY) connected directly to a DVD Recorder (Magnavox, Phillips Corporation, Andover, MA) and oriented perpendicular to the bursal surface of the tendon. To track marker motion, images were first thresholded and converted to a binary format so that only the markers were visible (Fig. 3(*b*)). For each frame, marker centroids were computed (Fig. 3(*c*)) and the trajectory of the marker centroid was tracked over time. Trajectories were then spatially differentiated to calculate the deformation gradient, from which an estimate of the in-plane small strains could be computed [20]. All analysis was done using the tensile strains computed along the long axis of the tendon (parallel to the loading direction). Strain within the tendon was summarized by the average and variance of strain (or translational motion) at the tendon's insertion site (across the cut, Fig. 4(*a*)) and the strain within the tissue proximal to the cut (Fig. 4(*b*)). To facilitate comparisons between the different specimens, we picked a common load (60 N) at which to compare the three strain measurements (grip-to-grip, tissue, and insertion). Strain values from each of the last three cycles were averaged. Three of the 7 mm deep defects and thirteen of the full thickness defects failed to reach 60 N of load during testing, so for those tests the strain at the maximum load was used.

2.6 Statistics. A repeated measures analysis of variance with cut location (e.g., bursal-sided cut) and cut depth (e.g., 33% thickness) as fixed effects and specimen as a random effect was performed on each of the three outcome measures (grip-to-grip

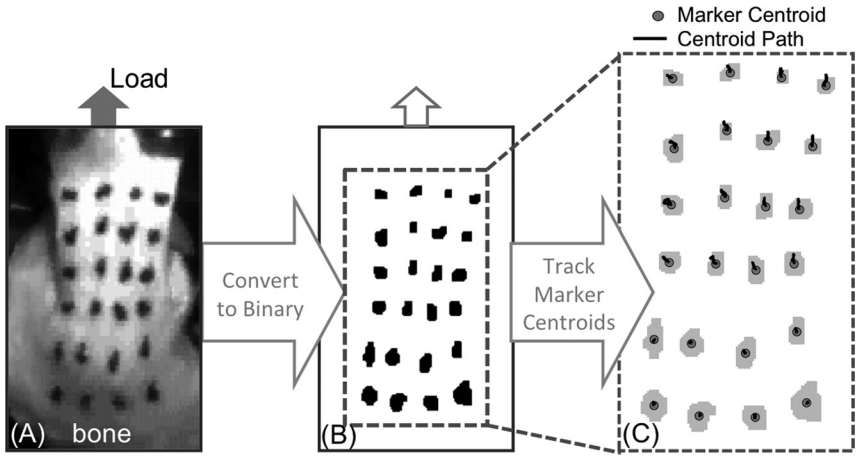

Fig. 3 Optical strain processing. (*a*) Tissue motion was imaged using markers placed on the bursal surface of the tendon (*b*) images were converted binary format to locate each marker in the imaging plane. (c) Marker centroid trajectories were tracked over time (centroid path). Displacements were then spatially differentiated to calculate strain in the tendon tissue.

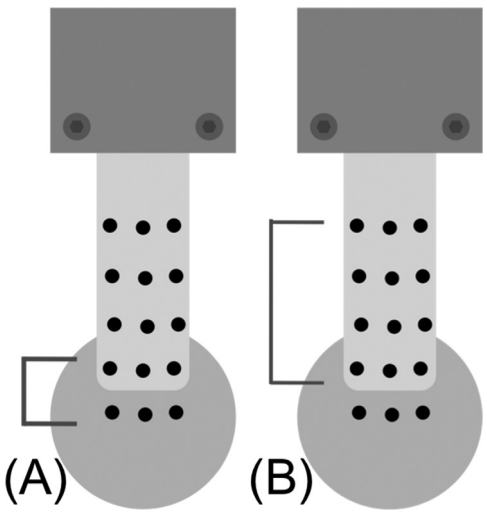

Fig. 4 Markers used for computing optical strain (*a*) at the insertion site, (*b*) within the tendon issue

strain, tissue strain, and insertion strain all at 60 N of external load). To standardize the measures for each specimen relative to the fully intact condition, the post hoc analyses presented are based on the paired differences from intact to the various depths of cut. Post hoc testing between the different cut locations at a given depth (e.g., articular versus bursal at 33% cut) was performed using Tukey HSD tests. Post hoc testing between the different cut severity for a given location (e.g., strain at 33% cut versus 66% cut for bursal) was also performed using Tukey HSD tests. Differences between each defect severity and intact for a given cut size/location (e.g., change in strain at 33% relative to intact for bursal) were assessed with Holm adjusted p-values from paired T-tests. Significance for all tests was set at $p = 0.05$. If the p-value was less than 0.1 the difference was consider a noticeable trend.

3 Results

3.1 Grip-to-Grip Strain. At a fixed load (60 N), the partial- and full-thickness cuts created from both the articular and bursal sides showed significant grip-to-grip strain increases when compared to the intact case (Figs. 5(*a*) and 5(*b*), Tables 1(*A*) and 1(*B*)). The bursal defect showed an increase of 1.1-fold for the 33% thickness defect and 1.2-fold for the 66% defect, while the articular group showed an increase of 1.1-fold for the 66% thickness defect. The full-thickness defects also experienced significantly greater grip-to-grip strain (a 1.4-fold increase for both groups) than the corresponding partial-thickness defects. Additionally, the bursal-sided defect exhibited a greater grip-to-grip strain change relative to the intact case ($p < 0.1$ for the 33% cut and $p < 0.05$ for the 66% cut—Fig. 6(*a*), Table 2).

3.2 Insertion Strain. Strains across the insertion site (Fig. 4(*a*)) demonstrated trends similar to the grip-to-grip strain (Figs. 5(*c*) and 5(*d*), Tables 1(*C*) and 1(*D*)). The 33% and 66% partial thickness defects increased the strain 2.4-fold and 4.8-fold, respectively, and the full-thickness defect increased strain sixfold. All of these changes were significant compared to the intact tendon. For the defect created on the articular side, the 33% partial thickness cuts did not change the observed strain significantly (no increase). The two-thirds thickness articular defect caused a statistically significant 1.3-fold increase and the full-thickness defect caused a statistically significant 6.6-fold increase. As with the grip-to-grip strain, the bursal strain increased more than articular strain for both the partial-thickness defects (Fig. 6(*b*), Table 2).

3.3 Tissue Strain. The tissue strains (Fig. 4(*b*)) showed different trends than the grip-to-grip and the insertion strains. No depth of bursal-sided defect showed significant differences relative to the intact tendon strain, while the partial-thickness articular-sided defects caused significant strain increases of 2.3-fold relative to the intact (Figs. 5(*e*) and 5(*f*), Tables 1(*E*) and 1(*F*)). For both the bursal and the articular defect groups the tissue strain also dropped to near zero after creation of the full-thickness defect (decreases of 10.3 and 4.3-fold, respectively). The 4.4-fold decrease in tissue strain for the 66% cut bursal-sided group was also a significant difference from the 2.3-fold increase in tissue strain experienced by the 66% thickness articular-sided cut (Fig. 6(*c*), Table 2).

4 Discussion

The purpose of this study was to investigate the influence of partial thickness tear location on mechanical strain distributions within the infraspinatus tendon. We did this by artificially introducing tendon cuts on the bursal and articular sides of intact tendon, and then assessing how strain patterns were altered within the tissue and near the tendon insertion. The most salient finding

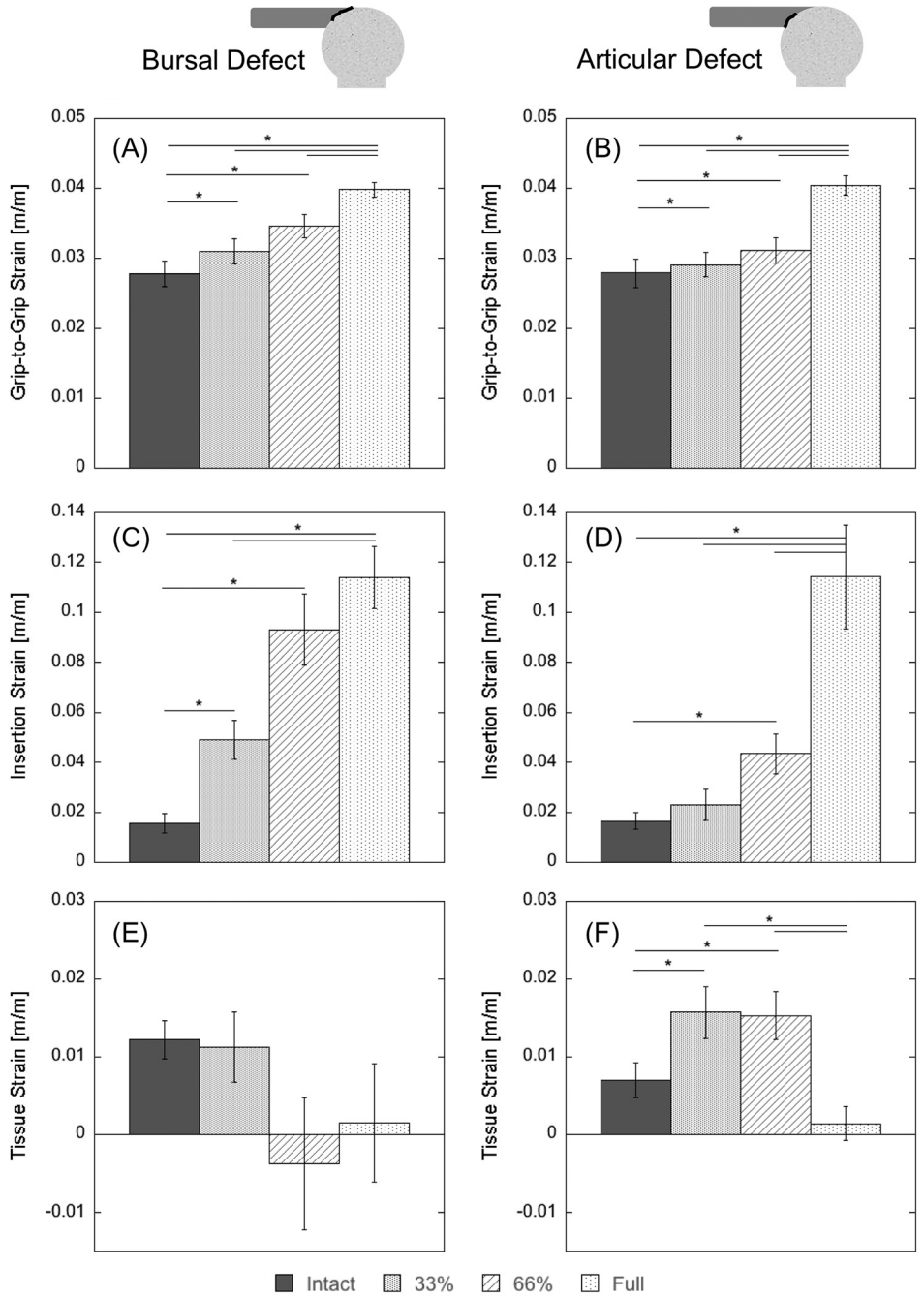

Fig. 5 Strain results by defect group. {Average (±1SE) strain at 60 N load for large bursal and articular defects. Grip-to-grip strains for (*a*) the bursal-sided defect (BS) and (*b*) articular-sided defect (AS) are significantly ($p < 0.05$) greater than intact for all cut depths. Insertion strain for (*c*) the BS group and (*d*) the AS group show even more dramatic increases with cut depth. Tissue strain for (*e*) the BS group does not change significantly for any cut, though the average does decrease to nearly zero for 66% and full-thickness cuts. Conversely, tissue strain increases significantly for both articular-sided cuts before dropping to nearly zero for the full-thickness cut. A summary of *P*-values is shown in Table 1. The * indicates a statistically significant ($p < 0.05$) difference between the two groups.

of the study was the observation that bursal-sided defects have a significantly greater effect on both overall and localized bursal-surface tissue strains than do articular defects. These altered strain levels may more readily contribute to tear propagation, and thus may relate to the clinical observation that bursal-sided defects often do not respond well to conservative (nonsurgical) treatment [5,9].

We hypothesized that defects initiated on the bursal side of the tendon would increase overall tendon strain more than articular sided defects. This hypothesis was confirmed with bursal-sided partial thickness defects inducing a greater increase in grip-to-grip strain than the corresponding articular-sided partial-thickness defects (Figs. 5(*a*), 5(*b*), 6(*a*)). This suggests that the intact tendon is carrying proportionally more of the load in the bursal side fibers than in the articular fibers. Recent studies of human supraspinatus tendon have discovered substantial variations in tissue stiffness and ultimate tensile stress throughout the tendon [12–14], with transverse stiffness being substantially greater on the bursal side relative to the articular side [21]. These spatial variations in tissue

Table 1 P-values for strain comparisons by group. Grip-to-grip strain: (A) Bursal-sided group. (B) Articular-sided group. Optical insertion strain: (C) Bursal-sided group. (D) Articular-sided group. Optical tissue strain: (E) Bursal-sided group and (E) articular-sided group. For each cut condition relative to intact *p*-values were calculated using a Holm adjusted Bonferroni comparison to account for the multiple comparisons. For the comparisons between other cut conditions adjusted *p*-values were calculated using a Tukey HSD test.

(A) Grip-to-grip (Bursal)

	Intact	33%	66%	Full
Intact	—	**0.007**	**0.002**	**<0.001**
33%		—	0.079	**<0.001**
66%			—	**0.008**
Full				–

(B) Grip-to-grip (Articular)

	Intact	33%	66%	Full
Intact	—	**0.002**	**0.001**	**<0.001**
33%		—	0.215	**<0.001**
66%			—	**<0.001**
Full				—

(C) Optical insertion (bursal)

	Intact	33%	66%	Full
Intact	—	**0.008**	**0.001**	**<0.001**
33%		—	**0.034**	**0.002**
66%			—	0.428
Full				—

(D) Optical insertion (articular)

	Intact	33%	66%	Full
Intact	—	0.407	**0.024**	**0.007**
33%		—	0.55	**<0.001**
66%			—	**0.004**
Full				—

(E) Optical insertion (bursal)

	Intact	33%	66%	Full
Intact	—	0.749	0.2	0.415
33%		—	0.258	0.552
66%			—	0.84
Full				—

(F) Optical tissue (articular)

	Intact	33%	66%	Full
Intact	—	**0.020**	**0.023**	0.168
33%		—	0.995	**0.005**
66%			—	**0.007**
Full				—

properties were strongly correlated with fiber alignment [21], which suggests that a similar presence of spatial variation in fiber architecture for sheep infraspinatus tendon could contribute to the differential strain effects we observed in response to cuts originating on the bursal and articular sides. Furthermore, if we extrapolate our differential strain results from sheep infraspinatus to human supraspinatus tendon, the greater reliance on the bursal-side fibers to bear load may in part explain why bursal-sided rotator cuff tears do not respond well to conservative treatment. In particular, a partial bursal sided tear may compromise the integrity of fibers on that side of the tendon leading to greater strain on the articular sided tissue. These larger strains contribute to a higher likelihood of tear propagation [9]. In addition, differential strain between layers of the tendon could contribute to tear propagation. A recent cross-sectional ultrasonography study shows a greater occurrence of partial thickness tears seeming to arise at the junction between the supraspinatus and infraspinatus tendons [22], where differential strain patterns might be expected to arise.

We also hypothesized that tissue adjacent to the tear would be subjected to reduced load, while tissue on the opposite side of the tear would exhibit signs of increased loading. This hypothesis was also confirmed, with the bursal sided tissue strain decreasing in response to bursal sided tears. For example, tissue strain on the bursal surface drops to approximately zero once the defect is 66% of the tendon thickness and stays there for the full thickness defect. In contrast, the strain across the insertion site (Figs. 5(*c*), 5(*d*), 6(*b*)) increased substantially with bursal sided defects as a result of a gapping effect occurring across tear. The close correspondence of the grip-to-grip and insertion strain patterns demonstrates that the overall stretch is dominated by the translational motion occurring at the tear. Conversely for the articular defect, the bursal-surface tissue strain increases significantly as soon as the tissue is cut from the articular side. The increase in bursal-sided tissue strain for the articular cut demonstrates that the strain

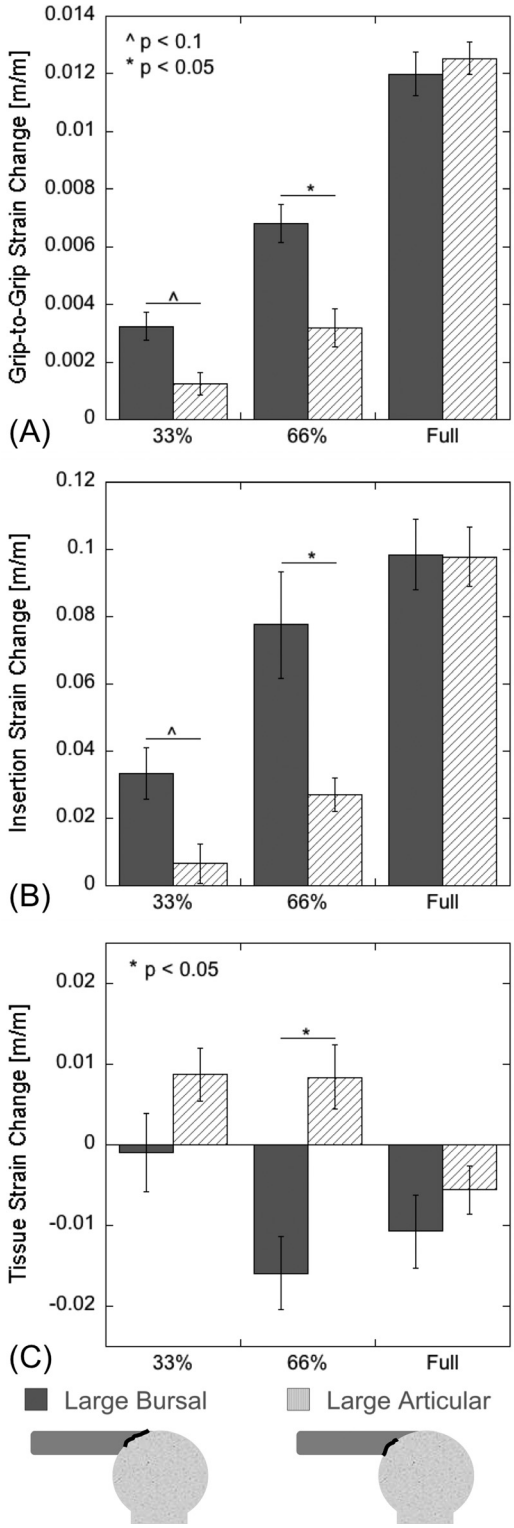

Fig. 6 Change in average (±1 SE) strain measures (at 60 N of load) due to 33%, 66%, and full thickness cuts. Bursal-sided partial defects compromised overall tendon stiffness more than articular sided defects, resulting in more significant increases in grip-to-grip and tissue strain. Changes in insertion strains were substantially smaller for both bursal and articular differences. *P*-values are shown in Table 2.

in the intact tissue adjacent to the cut increases. These findings are consistent with previous studies [10–12].

The limitations of this study should be considered when applying the results to clinically observed rotator cuff tendon tears.

Table 2 *P*-values comparing bursal and articular defect group strain changes. For the comparisons between the defect groups at each cut condition, adjusted *p*-values were calculated using a Tukey HSD test.

	33% Cut	66% Cut	Full Cut
Grip-to-grip	0.093	**0.032**	0.975
Optical insertion	0.095	**0.02**	1
Optical tissue	0.218	**0.011**	0.898

First, we created the tears artificially by using a razor blade in an ex-vivo model. While this does achieve the loading conditions of a tear, it fails to mimic the pathologic and degenerative changes that are usually associated with a rotator cuff tendon tear. Second, we used a sheep infraspinatus tendon, which is frequently used as a model for rotator cuff pathology repair due to its size and geometric similarity to the human supraspinatus tendon; however, it has recently been suggested that smaller mammals or rodents may be a more functionally accurate model [23,24]. In addition, it has recently been reported that collagen fiber organization and alignment are affected by load; however, little work has been done comparing the fibril level architecture between sheep and human rotator cuff tendons, which limits the inferences that can be made [14,17,21]. Third, the present study measured strain only on the bursal surface of the tendon, and while strain on the bursal surface is greater with bursal defects compared to articular defects, this does not explicitly prove that the insertion strain on the articular side of the tendon is less for an articular defect. It would be valuable and applicable to measure strain throughout the tendon, particularly in the deep substance, in order to better understand the effects of partial-thickness defects [11,25]. Finally, the resolution of strain measurements was limited by the marker spacing (about 5 mm). Ideally, it would be possible to measure strain immediately around the defect and to divide the tissue into cut and un-cut regions.

In conclusion, we have found that cutting the bursal fibers of a sheep infraspinatus tendon causes a greater decrease in strain at 60 N of load compared to the strain change resulting from cutting the articular fibers, which suggests that more of the load is carried by the bursal fibers. This finding may help to explain why bursal-sided tears respond poorly to conservative treatment. Our data also show that the average bursal-surface strain in tendon tissue reflects a local strain effect in the tissue, with the strain decreasing when measured adjacent to a partial-thickness cut and increasing when measured on the opposite side from the cut. Finally, our data shows that strain across the insertion site increases for a defect created at the insertion site on either the bursal or the articular side, though the apparent strain increases when the cut is on the same side as the measurement is likely due to gapping.

Acknowledgment

Contributions by Kim Safarik, Liz Vincent, Kurt Frisch, Ellen Leiferman, Ron McCabe, Scott Hetzel, and the UW Orthopedics Resident Research Program are acknowledged. Research reported in this publication was supported by the National Institute of Arthritis and Musculoskeletal and Skin Diseases of the National Institutes of Health under Award Number AR059916 and AR056201. The content is solely the responsibility of the authors and does not necessarily represent the official views of the National Institutes of Health.

References

[1] Soslowsky, L. J., Carpenter, J. E., Bucchieri, J. S., and Flatow, E. L., 1997, "Biomechanics of the Rotator Cuff," Orthop. Clin. North Am., **28**(1), pp. 17–30.
[2] Perry, S. M., Getz, C. L., and Soslowsky, L. J., 2009, "After Rotator Cuff Tears, the Remaining (Intact) Tendons are Mechanically Altered," J. Shoulder Elb. Surg. Am. Shoulder Elb. Surg. Al., **18**(1), pp. 52–57.
[3] Breazeale, N. M., and Craig, E. V., 1997, "Partial-Thickness Rotator Cuff Tears. Pathogenesis and Treatment," Orthop. Clin. North Am., **28**(2), pp. 145–155.
[4] McConville, O. R., and Iannotti, J. P., 1999, "Partial-Thickness Tears of the Rotator Cuff: Evaluation and Management," J. Am. Acad. Orthop. Surg., **7**(1), pp. 32–43.
[5] Fukuda, H., Hamada, K., Nakajima, T., Yamada, N., Tomonaga, A., and Goto, M., 1996, "Partial-Thickness Tears of the Rotator Cuff. A Clinicopathological Review Based on 66 Surgically Verified Cases," Int. Orthop., **20**(4), pp. 257–265.
[6] Flatow, E. L., Altchek, D. W., Gartsman, G. M., Iannotti, J. P., Miniaci, A., Pollock, R. G., Savoie, F., and Warner, J. J., 1997, "The Rotator Cuff. Commentary," Orthop. Clin. North Am., **28**(2), pp. 277–294.
[7] Peterson, C. A., and Altchek, D. W., 1986, "Arthroscopic Treatment of Rotator Cuff Disorders," Clin. Sports Med., **15**(4), pp. 715–736.
[8] Weber, S. C., 1999, "Arthroscopic Debridement and Acromioplasty Versus Mini-Open Repair in the Treatment of Significant Partial-Thickness Rotator Cuff Tears," Arthrosc. J. Arthrosc. Relat. Surg. Off. Publ. Arthrosc. Assoc. N. Am. Int. Arthrosc. Assoc., **15**(2), pp. 126–131.
[9] Andarawis-Puri, N., Ricchetti, E. T., and Soslowsky, L. J., 2009, "Rotator Cuff Tendon Strain Correlates With Tear Propagation," J. Biomech., **42**(2), pp. 158–163.
[10] Reilly, P., Amis, A. A., Wallace, A. L., and Emery, R. J. H., 2003, "Mechanical Factors in the Initiation and Propagation of Tears of the Rotator Cuff. Quantification of Strains of the Supraspinatus Tendon In Vitro," J. Bone Joint Surg. Br., **85**(4), pp. 594–599.
[11] Bey, M. J., Song, H. K., Wehrli, F. W., and Soslowsky, L. J., 2002, "Intratendinous Strain Fields of the Intact Supraspinatus Tendon: The Effect of Glenohumeral Joint Position and Tendon Region," J. Orthop. Res. Off. Publ. Orthop. Res. Soc., **20**(4), pp. 869–874.
[12] Nakajima, T., Rokuuma, N., Hamada, K., Tomatsu, T., and Fukuda, H., 1994, "Histologic and Biomechanical Characteristics of the Supraspinatus Tendon: Reference to Rotator Cuff Tearing," J. Shoulder Elb. Surg., **3**(2), pp. 79–87.
[13] Lee, S. B., Nakajima, T., Luo, Z. P., Zobitz, M. E., Chang, Y. W., and An, K. N., 2000, "The Bursal and Articular Sides of the Supraspinatus Tendon Have a Different Compressive Stiffness," Clin. Biomech. Bristol Avon, **15**(4), pp. 241–247.
[14] Lake, S. P., Miller, K. S., Elliott, D. M., and Soslowsky, L. J., 2009, "Effect of Fiber Distribution and Realignment on the Nonlinear and Inhomogeneous Mechanical Properties of Human Supraspinatus Tendon Under Longitudinal Tensile Loading," J. Orthop. Res. Off. Publ. Orthop. Res. Soc., **27**(12), pp. 1596–1602.
[15] Yang, S., Park, H.-S., Flores, S., Levin, S. D., Makhsous, M., Lin, F., Koh, J., Nuber, G., and Zhang, L.-Q., 2009, "Biomechanical Analysis of Bursal-Sided Partial Thickness Rotator Cuff Tears," J. Shoulder Elb. Surg. Am. Shoulder Elb. Surg. Al., **18**(3), pp. 379–385.
[16] Mazzocca, A. D., Rincon, L. M., O'Connor, R. W., Obopilwe, E., Andersen, M., Geaney, L., and Arciero, R. A., 2008, "Intra-Articular Partial-Thickness Rotator Cuff Tears: Analysis of Injured and Repaired Strain Behavior," Am. J. Sports Med., **36**(1), pp. 110–116.
[17] Gerber, C., Schneeberger, A. G., Beck, M., and Schlegel, U., 1994, "Mechanical Strength of Repairs of the Rotator Cuff," J. Bone Joint Surg. Br., **76**(3), pp. 371–380.
[18] Turner, A. S., 2007, "Experiences With Sheep as an Animal Model for Shoulder Surgery: Strengths and Shortcomings," J. Shoulder Elb. Surg. Am. Shoulder Elb. Surg. Al., Suppl. **16**(5), pp. S158–S163.
[19] Clavert, P., Kempf, J. F., Bonnomet, F., Boutemy, P., Marcelin, L., and Kahn, J. L., 2001, "Effects of Freezing/Thawing on the Biomechanical Properties of Human Tendons," Surg. Radiol. Anat. SRA, **23**(4), pp. 259–262.
[20] Weiss, J. A., and Gardiner, J. C., 2001, "Computational Modeling of Ligament Mechanics," Crit. Rev. Biomed. Eng., **29**(3), pp. 303–371.
[21] Lake, S. P., Miller, K. S., Elliott, D. M., and Soslowsky, L. J., 2010, "Tensile Properties and Fiber Alignment of Human Supraspinatus Tendon in the Transverse Direction Demonstrate Inhomogeneity, Nonlinearity, and Regional Isotropy," J. Biomech., **43**(4), pp. 727–732.
[22] Kim, H. M., Dahiya, N., Teefey, S. A., Middleton, W. D., Stobbs, G., Steger-May, K., Yamaguchi, K., and Keener, J. D., 2010, "Location and Initiation of Degenerative Rotator Cuff Tears: An Analysis of Three Hundred and Sixty Shoulders," J. Bone Joint Surg. Am., **92**(5), pp. 1088–1096.
[23] Coleman, S. H., Fealy, S., Ehteshami, J. R., MacGillivray, J. D., Altchek, D. W., Warren, R. F., and Turner, A. S., 2003, "Chronic Rotator Cuff Injury and Repair Model in Sheep," J. Bone Joint Surg. Am., **85A**(12), pp. 2391–2402.
[24] Mathewson, M. A., Kwan, A., Eng, C. M., Lieber, R. L., and Ward, S. R., 2013, "Comparison of Rotator Cuff Muscle Architecture Among Humans and Selected Vertebrate Species," J. Exp. Biol., **217**(Pt. 2), pp. 261–273.
[25] Bey, M. J., Ramsey, M. L., and Soslowsky, L. J., 2002, "Intratendinous Strain Fields of the Supraspinatus Tendon: Effect of a Surgically Created Articular-Surface Rotator Cuff Tear," J. Shoulder Elb. Surg. Am. Shoulder Elb. Surg. Al., **11**(6), pp. 562–569.